CHAPTER 4

PERFORMANCE ENHANCEMENT OF REGENERATIVE EVAPORATIVE COOLER

4.1 Introduction

The heat and mass transfer of a regenerative heat and mass exchanger (HMX) can be increased by passive techniques. The use of nanofluid and modification of the heat transfer surfaces are beneficial techniques in the direction of performance enhancement. The use of the nano particles in the coolant (water) improves the thermophysical properties, which will improve the heat transfer coefficients. The use of the Nano particles can also improve the evaporation rate and heat and mass transfer coefficient (Moghiman et al., 2013). Hence the use of nano fluid in an evaporative cooler enhances the performance (Tariq et al., 2018). Furthermore, the modified plate surfaces enhance the heat and mass transfer due to dual effects of an increase in surface area and heat transfer coefficients.

The literature shows that apart from the flat surface, finned, baffled, and corrugated surfaces were used in REC. Plenty of studies has been done on the plate heat exchanger by modifying the surface (by corrugation or embossing) or by increasing the roughness of the surface. There are many other surface modifications that can be used in REC, such as asterisk surface (Durmuş et al., 2009), capsule embossing, which has a shape close to ellipsoidal (Monteiro et al., 2015), and small-sized protruding finned surface (Zhang et al., 2016); however, they have not been studied by researchers. Furthermore, the hybrid nanofluids have emerged recently as an advanced heat transfer fluid (Sarkar et al., 2015); however, these were not used in REC.

Hence, in the present investigation, an attempt has been made to investigate the performance of the regenerative HMX by using various water-based hybrid nanofluids as coolant and surface modifications (capsule embossing, fin, and corrugation). First, the performance (cooling capacity, dew point effectiveness, coefficient of performance, and exergy efficiency) of regenerative HMX has been compared using various hybrid nanofluids. Then, the water consumption rate and other parameters have been compared between different cooling plate surface modifications by varying the operating parameters (inlet dew-point depression, air inlet velocity, and coolant flow rate).

4.2. Modeling and simulation

The layout of REC (chosen best flow configuration according to the study present in previous chapter studies) and considered surface modifications are shown in Figs. 4.1 and 4.2, respectively. As shown in Fig. 4.1, the air intake to the device takes place at point 1. The total air (supply + exhaust) in dry channels exchanges sensible heat with the adjacent wet channels. Then a fraction of the dry channel air is redirected in the wet channel while the rest is supplied to the conditioning space at point 2. The exhaust air flows over the cooling wet material and exits the device at point 3.

The considered surface modifications with geometric specifications are shown in Fig.4 2. The length of the capsule is 12 mm, and the width is 10 mm. the capsule height is 2.5 mm. The fin has 5 mm in width and the same height as the gap between the two plates. The plate pitch to corrugation pitch ratio (p_p/p_c) ratio is taken as 0.25.

There is sensible heat transfer in the dry air side, latent heat transfer in the wet air side, and mass transfer of water occurs in the wet channel. The cooler has been discretized lengthwise, and the conservation equations of energy and mass in the channels are used for each differential element with some simplifications (as discussed in chapter 3).

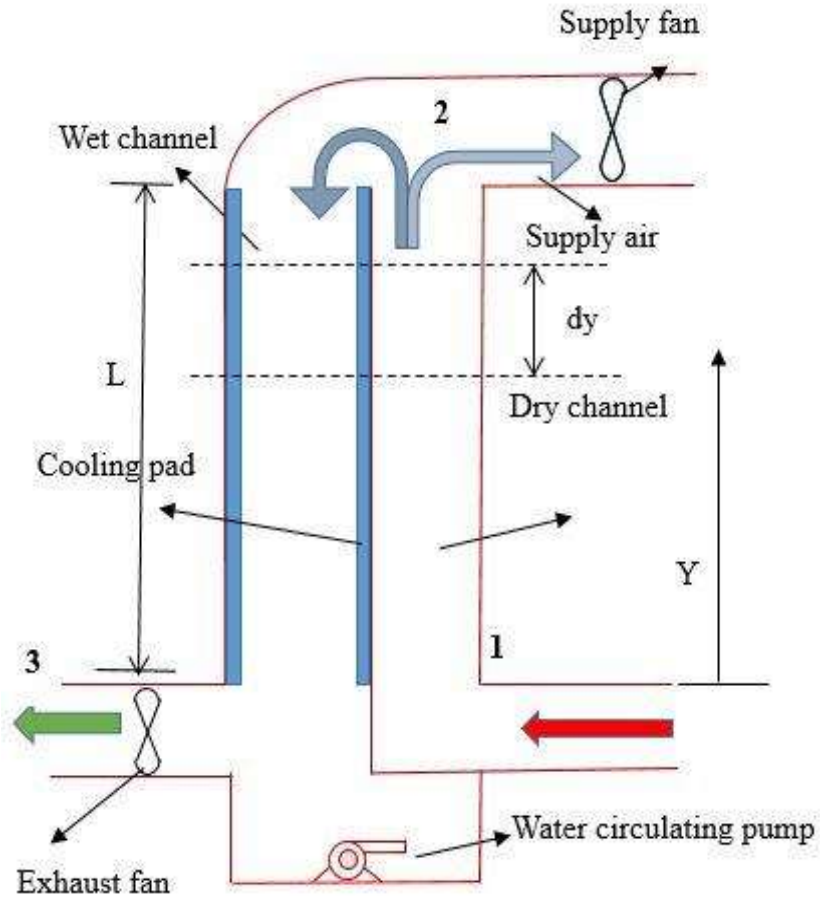

Fig. 4.1 Counter-flow regenerative evaporative cooler

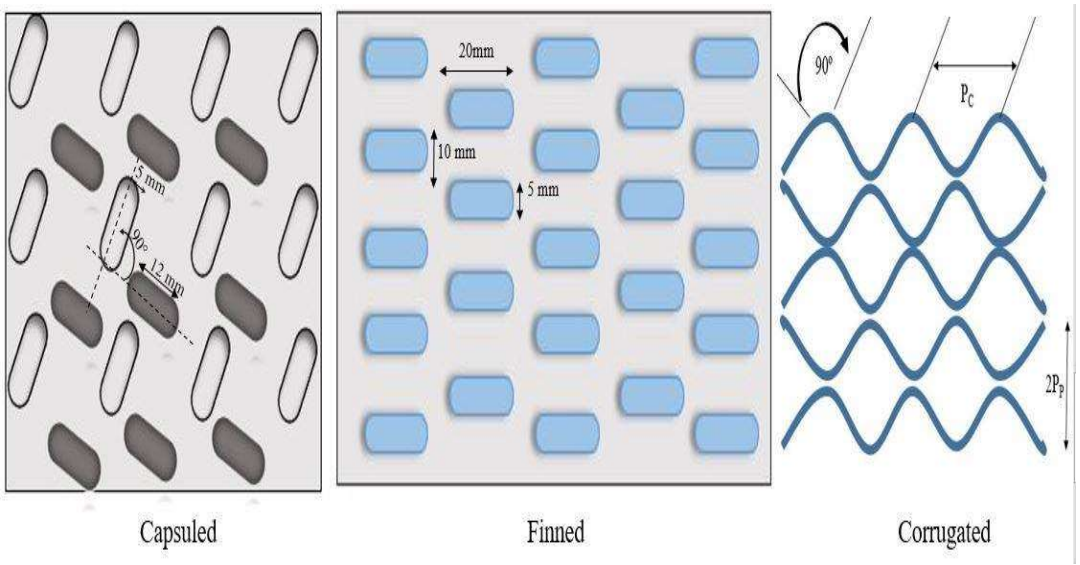

Fig. 4.2 Modified surface profiles (capsule embossing, finned and corrugated surfaces)

4.2.1 Correlations used for the surface modifications

As both channel air velocity and hydraulic diameter are low, the flow regime is laminar. The Reynolds number at the mean condition is 1202. With the variation of the intake velocity, Reynolds number varies in the range of 601-1804, which is in the laminar zone. The Nusselt number for fully developed forced convection laminar can be divided into two regions (undeveloped length (= $0.05\mathrm{RePrD_h}$) and fully developed length). Hence, for the air in the dry channel, the average Nusselt number, based on the channel length (L) by combining the underdeveloped and fully developed regions, has been used. By neglecting the dynamic viscosity deviation between bulk to wall temperatures, the Nusselt number for the entrance region of regenerative EC with the flat plate is given by (Zhan et al., 2011),

$$Nu = 1.86\left(\mathrm{Re}\,\mathrm{Pr}\,d_h/L\right)^{1/3} \tag{4.1}$$

The dry channel developed region air flow, the Nusselt number can be calculated with the help of correlation as presented below:

The regenerative HMX of flat plate (Riangvilaikul et al., 2010), $Nu = 8.235$ (4.2)

The regenerative HMX of capsule embossing (Zhang et al., 2016),

$$Nu = 0.655Re^{0.581}Pr^{0.317} \tag{4.3}$$

The regenerative HMX of fin type (Monteiro et al., 2012), $\dfrac{NuPr^{-1/3}}{Re} = 0.590Re^{-0.543}$ (4.4)

The regenerative HMX of corrugated type (Lee et al., 2013), $Nu = (8.235^3 + Nu_t^3)^{1/3}$ (4.5)

$$\text{Where } Nu_t = \{0.0205 + 1.15(\frac{p_p}{p_c})^{1.18}\}Re^{0.8-0.2(\frac{p_p}{p_c})} \tag{4.6}$$

The Nusselt number for secondary air channels for regenerative HMX is given by [28],

$$Nu = 2 + 0.6Re^{0.5}Pr^{0.33} \tag{4.7}$$

Where $Re = \frac{\rho_{pa} d_h u_{pa}}{\mu_{pa}}$ (for dry air), and $Re = \frac{\rho_{sa} d_h u_{ra}}{\mu_{sa}}$ (for wet air).

The relative air velocity flow has been used to consider the directional effect of air and water. The primary and secondary channel heat transfer coefficients are calculated using, respectively,

$$\alpha_{pa} = Nu\left(k_{pa} / d_{h,pa}\right) \tag{4.8}$$

$$\alpha_{sa} = Nu\left(k_{sa} / d_{h,sa}\right) \tag{4.9}$$

The supply air and exhaust air make a combined entry in the device, as shown in Fig. 4.3. The total fan power is the summation of the supply fan and exhaust fan. The individual pressure drop of supply air (dry air) and exhaust air (working air) is calculated theoretically, and the respective volume flow rate is multiplied to calculate fan power consumption. The pressure drop of dry channel air comprises of internal (frictional) pressure drop and external (sudden contraction, bend, line flow, and outlet expansion losses) pressure drop, and written as (Duan et al., 2017),

$$\Delta p_{pa} = f \frac{\rho_{pa} u_{pa}^2}{2 d_h} L + \sum \zeta \frac{\rho_{pa} u_{pa}^2}{2} \tag{4.10}$$

The average friction factor for a flat plate is given by (Duan et al., 2017),

$$f = \frac{4}{Re}\left[\frac{3.44}{\sqrt{l^+}} + \frac{\frac{1.25}{4l^+} + \frac{f_{fd} Re}{4} - \frac{3.44}{\sqrt{l^+}}}{1 + \frac{0.00021}{\left(l^+\right)^2}}\right] \tag{4.11}$$

Where $l^+ = \frac{L}{d_h Re}$ and friction factor for HMX having a flat surface (fully developed) is

$$f = \frac{96}{Re} \text{ (Incropera et al., 2007)} \tag{4.12}$$

Friction factor capsule embossed HMX (Zhang et al., 2016) is $f = 1.041 Re^{-0.378}$ (4.13)

The friction factor of fin-type HMX (Monteiro et al., 2012) is $f = 0.973Re^{-0.456}$ (4.14)

The friction factor of corrugated HMX (Lee et al., 2013) is $f = (f_l^3 + f_t^3)^{1/3}$ (4.15)

Where $f_l = 2.42(\frac{p_p}{p_c}) + \frac{96 + 542\frac{p_p}{p_c}}{Re}$ and $f_t = \{0.184 + 14.9(\frac{p_p}{p_c})^{1.4}\}Re^{-0.2+0.046\frac{p_p}{p_c}}$

Where p_p / p_c is the ratio of plate pitch to corrugation pitch, In this simulation, it is taken as 0.25.

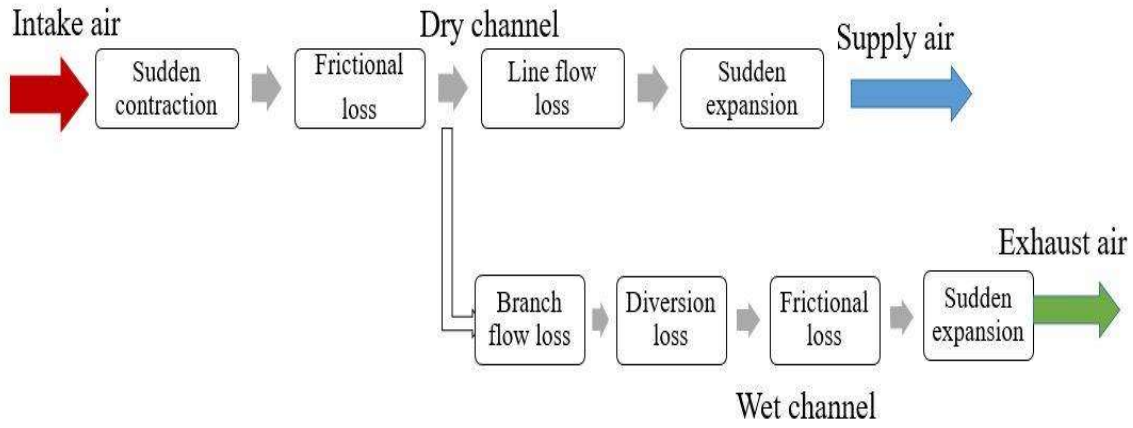

Fig. 4.3: Line diagram for air pressure loss in regenerative evaporative cooler

4.2.2 Nanofluid and its thermophysical property

The nono fluid contains nano-sized metal particles suspended in the base fluid. It enhances the heat transfer property between the surface and the heat transfer medium. The thermophysical properties, such as thermal conductivity and specific heat, play an important role in heat transfer. The hybrid nanofluid proved to be significant and more advantageous in this heat transfer enhancement (Sarkar et al., 2015). Following water-based hybrid Nanofluids are used in place of water with 1% nanoparticle volume concentration:

(a)- Aluminum oxide + Silicon carbide (50/50)

(b)- Aluminum oxide + Copper (50/50)

(c)- Aluminum oxide +Silver (50/50)

(d)- Aluminum oxide + Titanium dioxide (50/50)

(e)- Aluminum oxide + MWCNT (50/50)

(f)- Aluminum oxide + Graphene (50/50)

The properties of these nanoparticles are listed in Table 4.1. The density of the nanofluids is calculated as:

$$\rho_{nf} = \phi_{p1}\rho_{p1} + \phi_{p2}\rho_{p2} + (1-\phi)\rho_w \tag{4.16}$$

Where p1 and p2 represent first and second nanoparticles, respectively and $\phi = \phi_{p1} + \phi_{p2}$. The specific heat of the hybrid nanofluid is calculated as:

$$\rho_{nf} c_{p,nf} = \phi_{p1}\rho_{p1}c_{p,p1} + \phi_{p2}\rho_{p2}c_{p,p2} + (1-\phi)\rho_w c_{p,w} \tag{4.17}$$

The thermal conductivity of the hybrid nanofluid is calculated as (Sahu and Sarkar, 2019):

$$k_{nf} = \left(\phi_{p1}k_{nf,p1} + \phi_{p2}k_{nf,p2}\right)/\phi \tag{4.18}$$

Where,

$$\frac{k_{nf,p}}{k_w} = \frac{k_p + 2k_w + 2\phi(k_p - k_w)}{k_p + 2k_w - \phi(k_p - k_w)} \quad \text{(for spherical shape)} \tag{4.19}$$

$$\frac{k_{nf,p}}{k_w} = \frac{k_p + 3.9k_w + 3.9\phi(k_p - k_w)}{k_p + 3.9k_w - \phi(k_p - k_w)} \quad \text{(for cylindrical shape)} \tag{4.20}$$

$$\frac{k_{nf,p}}{k_w} = \frac{k_p + 4.7k_w + 4.7\phi(k_p - k_w)}{k_p + 4.7k_w - \phi(k_p - k_w)} \quad \text{(for platelet shape)} \tag{4.21}$$

The viscosity of the hybrid nanofluid is calculated as (Sahu et al., 2019),

$$\mu_{nf} = \left(\phi_{p1}\mu_{nf,p1} + \phi_{p2}\mu_{nf,p2}\right)/\phi \tag{4.22}$$

$$\frac{\mu_{nf,p}}{\mu_w} = 1 + 2.5\phi + 6.2\phi^2 \quad \text{(for spherical shape)} \tag{4.23}$$

$$\frac{\mu_{nf,p}}{\mu_w} = 1 + 13.5\phi + 904.4\phi^2 \quad \text{(for cylindrical shape)} \quad (4.24)$$

$$\frac{\mu_{nf,p}}{\mu_w} = 1 + 37.1\phi + 612.6\phi^2 \quad \text{(for platelet shape)} \quad (4.25)$$

MWCNT is assumed to be a cylindrical shape, Graphene is platelet shape, and other nanoparticles are spherical in shape. The respective correlation has been used to calculate the property.

Table 4.1: Thermophysical properties of considered nanoparticles

Nanoparticle	Density (kg/m^3)	Specific heat (J/kgK)	Thermal conductivity (W/mK)
alumina	3970	773	40
Silver	10500	235	429
Copper	8933	385	401
Silicon carbide	3160	1340	350
Titanium dioxide	4157	692	8.40
MWCNT	2600	3000	740
Graphene	2200	790	5000

4.2.3 Performance parameters

The important performance parameter is the sensible cooling capacity, dew point effectiveness (DPE), coefficient of performance (COP), and exergy efficiency are discussed in the earlier chapter. The amount of water evaporation is calculated as,

$$\dot{m}_{w,evaporated} = \dot{m}_{sa}(\omega_{sa,out} - \omega_{sa,in}) \quad (4.26)$$

Hence, the water consumption rate per unit cooling capacity can be written as,

$$\dot{m}_{w,consumption} = \frac{\dot{m}_{w,evaporated}}{Q_{system}} \tag{4.27}$$

4.2.4 Numerical solution and validation

The derived one-dimensional differential equations have been discretized with the help of the FDM (finite difference method) using the backward difference scheme. Then the discretized coupled differential equations of the mass and energy balances of the evaporative heat and mass exchanger have been implemented in the Engineering Equation Solver (EES) (Klein, 2017). The boundary conditions for the regenerative HMX are as follows: at bottom surface Y=0, $T_{pa} = T_{in}$; at top surface Y=L, $T_{sa} = T_{pa}$, $\omega_{sa} = \omega_{in}$, $T_w = T_{w,in}$. The air, water, and water vapor properties are calculated with in-built functions in the EES framework. Systems of equations are solved using a variation of Newton's method by EES. The equations are iteratively solved until the relative residuals fall below 10^{-6}. The performance of the REC is calculated after obtaining the properties at different discrete points along the length. The grid indecency test has been performed to check the influence of the number of nodes on the error of results. It is found that after 150 nodes, the variation of results is insignificant, and this has been further used for the analysis. The geometries of surface modifications are handled by using geometric-specific Nusselt number and friction factor correlations, taken from published papers. The results are presented for the fixed shape of the capsule, fin, and corrugation (fixed plate pitch to corrugation pitch).

The numerical simulation is validated with the experimental result of Duan et al. (2017), as shown in Table 4.2. The geometric dimensions of the heat exchanger are the gap between the plates = 3 mm, heat exchanger length = 0.86 m, heat exchanger width = 0.0458 m. The model simulated at : intake humidity ratio = 10.94 g/kg and 8.51 g/kg , intake air velocity 3.6 m/s, wet to dry air ratio = 0.47. The simulated result shows good

agreement with the experimental results. The numerical model is also validated with the test results of (Hasan 2010). The specifications of evaporative cooler used for this validation are: height of the wet channel = 0.0035 m, height of the dry channel = 0.0035 m, length of the HMX = 0.5 m, width of the HMX = 0.5 m, plate thickness = 0.2 mm. The reference operating conditions are: inlet temperature = 30°C, inlet humidity ratio = 0.009 kg/kg, inlet air flow rate= 0.0014 kg/s, extraction ratio = 0.70. Fig. 4.4 shows the temperature variation of air in the dry channel, air in the wet channel, the water film, and published results. Air temperature in the dry channel is fairly matched with (Hasan 2010) results with a maximum 3.2 % deviation. Hence, this validates the model and is used for further investigation with the addition of nanofluid and surface modification.

Table 4.2: Validation of simulated temperature with published experimental data

	Comparison of simulated result with published experimental data of the Duan et al. (2017)					
	Inlet humidity of = 8.51 g/kg			Inlet humidity of =10.94 g/kg		
Inlet temperature (ºC)	Simulation result	Experimental result	Error (%)	Simulation result	Experimental result	Error (%)
35.7	20.98	20.8	0.8	22.76	22.7	0.26
37.1	21.15	20.9	1.1	22.96	22.8	0.70
38	21.32	21.0	1.5	23.15	22.9	1.09
39	21.55	21.1	2.1	23.35	23.0	1.52
25	21.71	21.2	2.4	23.55	23.0	2.39

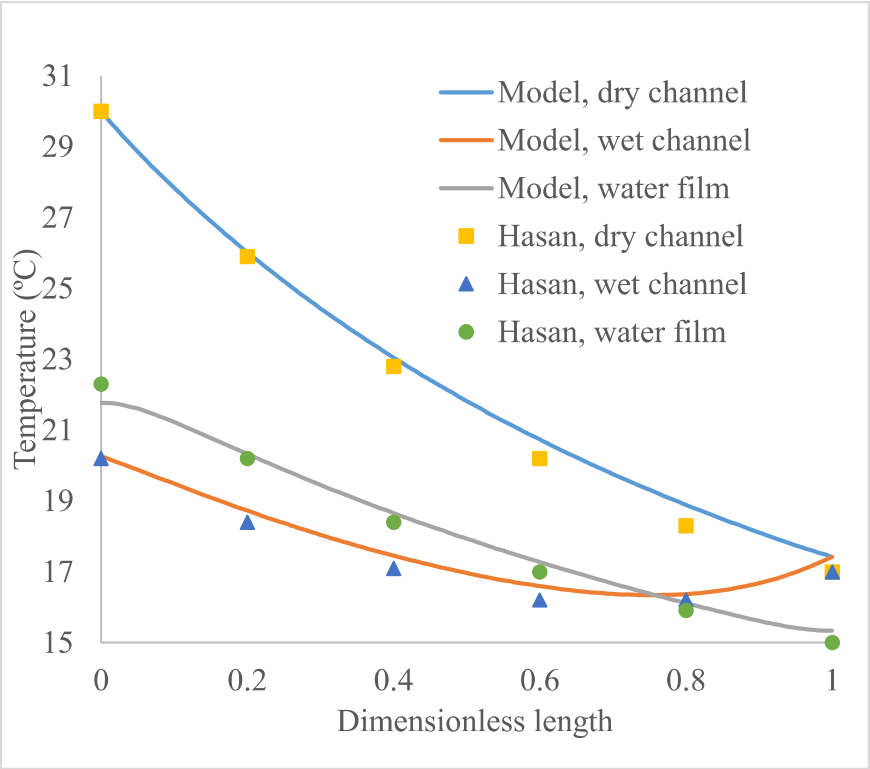

Fig. 4.4: Validation of the present numerical model for flat plate

4.3. Results and discussion

The considered geometrical specification of the REC and operating conditions are given in Table 4.3. Mean dry air inlet conditions: dry bulb temperature is 35 ºC, wet bulb temperature is 21.98 ºC, specific humidity is 11.2 g/kg, and the flow rate is 0.28 m^3/s. All the comparisons of the different surface modifications of regenerative HMX are made at the mean operating condition. The operating parameters (inlet wet-bulb depression temperature, inlet velocity, and water volume flow rate) are varied by keeping the other parameters constant. Type A is used for flat plate, B for capsule embossed plate, C for the finned plate, and D for the corrugated surface plate.

Table 4.3: Geometric and operating parameters (at mean conditions) of REC

Length of the channels of REC	1.20 m
Width of the REC	0.40 m
Height of the REC	0.70 m

Channel height (gap)	0.005 m
Plate thickness of the HMX	0.50 mm
Water flow rate per wet channel	5 L/h
Water inlet temperature	17 ºC
Wet air to dry air ratio	0.30
Inlet dry air velocity	2.0 m/s
Total numbers of channels pairs (dry and wet)	70

4.3.1 Hybrid nanofluid effect

The performance of flat plate type regenerative evaporative cooler is compared by using considered hybrid nanofluids at mean operating conditions. A small amount of reduction in the cooling temperature is achieved while using different hybrid nanofluids. The reduced temperature drop increases cooling capacity, as shown in Fig.4.5. There is no difference in the temperature of regenerative HMX between the different hybrid nanofluids due to the small volume fraction concentration of the nanoparticles in the base fluid. Fig. 4.6 compares the dew point effectiveness, and Fig. 4.7 compares the COP of the regenerative HMX at mean conditions. The improvement of 2.17 % is achieved in the dew point effectiveness while 2.14 % in the coefficient of performance with the application of the hybrid nanoparticles in the working fluid (water). This increase in exergetic performance is achieved due to an increase in the cooling effect. The result shows a similar trend for all the investigated performance parameters. This improvement in performance is achieved only due to improvement in the thermophysical property of the base fluid by adding different Nanoparticles to it. The Exergetic efficiency of the REC for all six different hybrid nanofluids and water as a base fluid is shown in Fig. 4.8. The REC with hybrid nanofluid shows high exergy efficiency than only water. The exegetic

efficiency varied very slightly with the different combinations of the nanoparticles. The highest Exergetic efficiency of 28.12% is obtained for alumina + MWCNT and the lowest for alumina + silver (28.07 %). The water consumption rate per unit cooling capacity increases slightly with the use of the hybrid nano particles in the regenerative evaporative cooler, as shown in Fig.4.9. The application of nanoparticles in the water affects the thermophysical property of the evaporative base fluid. The physics involvement includes movement of nanoparticles, wettability of nanofluid film, thermophoresis, and diffusiophoresis (Mahian et al., 2017), and Brownian motion. The mass transfer phenomena of the nanofluids are studied mostly experimentally in literature. Its mass diffusion behavior needs to investigate to understand its phenomena.

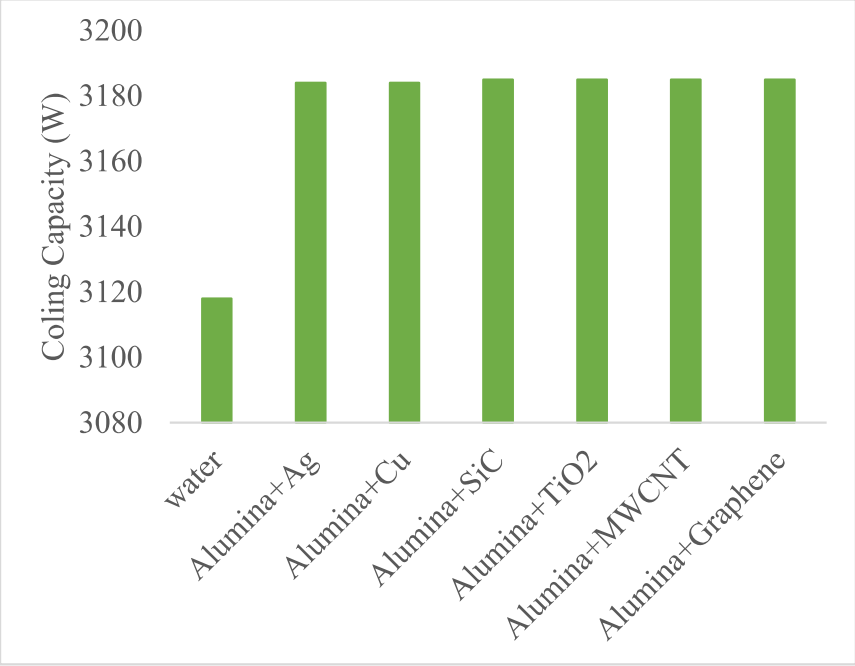

Fig. 4.5: Cooling capacity of REC with different hybrid nanofliuds

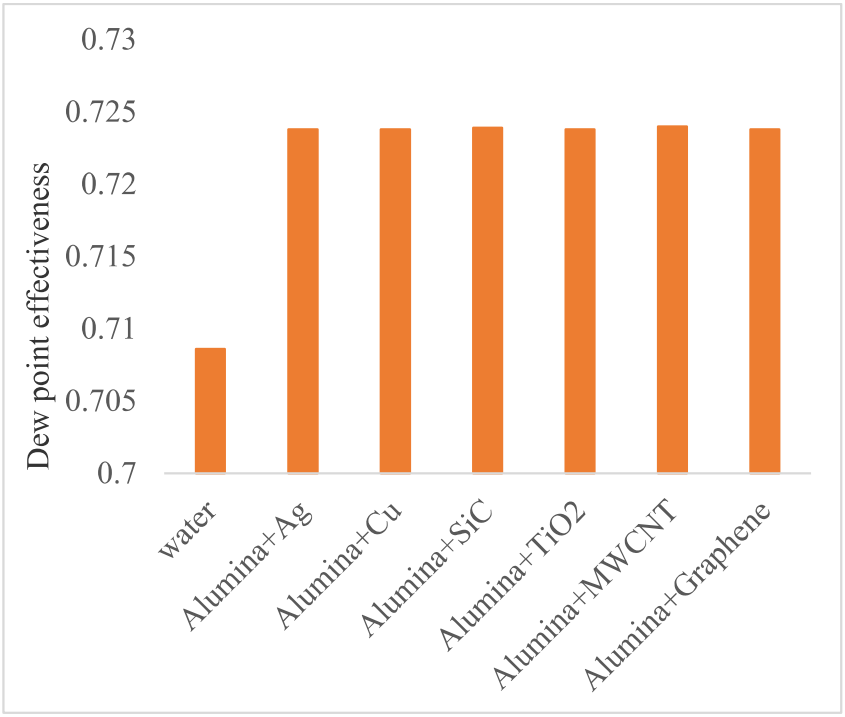

Fig. 4.6: Dew point effectiveness of REC with different hybrid nanofliuds

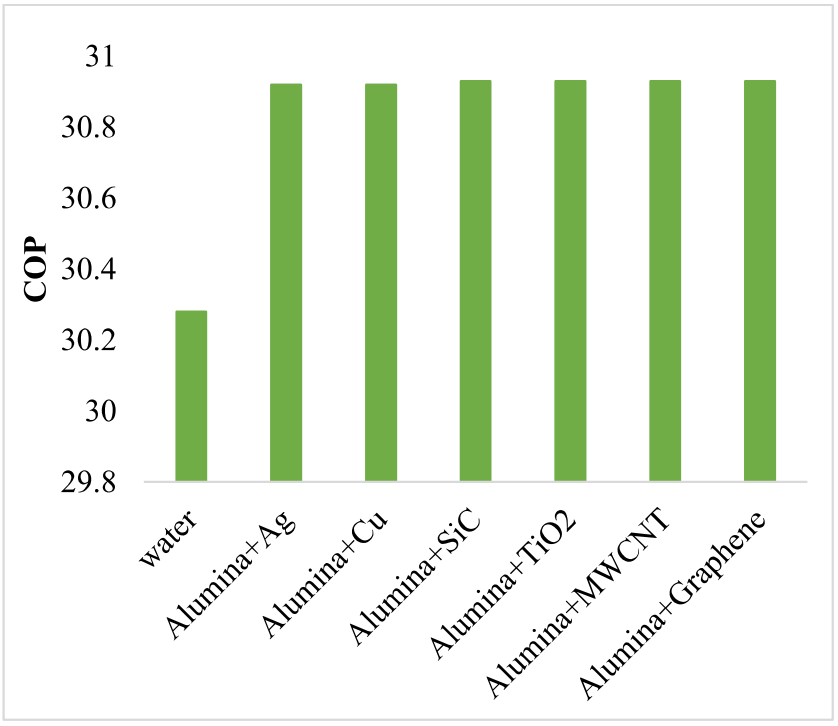

Fig. 4.7: COP of REC with different hybrid nanofliuds

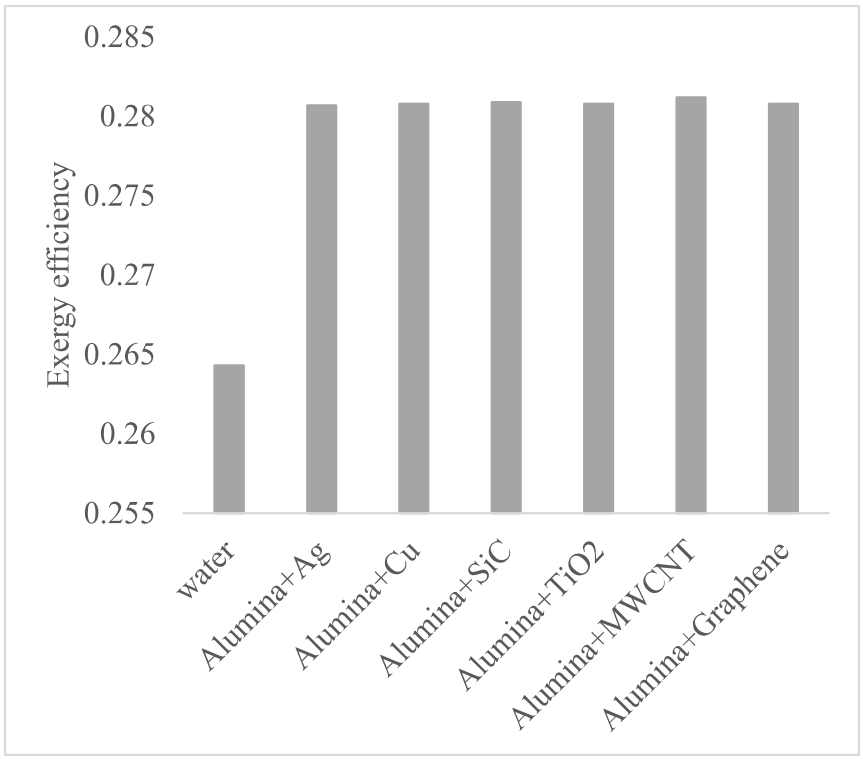

Fig. 4.8: Exergy efficiency of REC with different hybrid nanofliuds

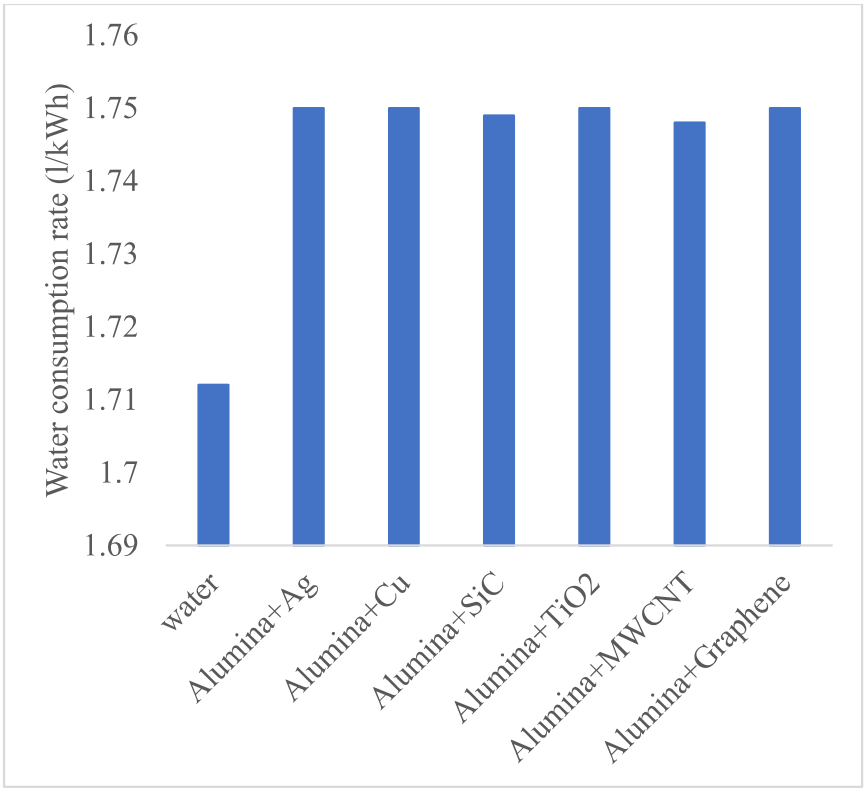

Fig. 4.9: Water consumption rate of REC with different hybrid nanofliuds

4.3.2 Influence of dew point depression

Fig. 4.10 shows the cooling capacity variation. The drier the outdoor air (at higher dew point depression), the higher would be the cooling capacity of the regenerative HMX for all types of modified surfaces. Fig. 4.11 shows the influence of inlet air dew point depression on effectiveness (DPE) for the four different surface modifications with the hybrid nanofluid. The higher dew point depression shows the high potential for evaporative cooling. The significant temperature drop occurs at a higher inlet depression for different types of surface modifications. The corrugated surface shows the highest effectiveness. The increase in the inlet dew point depression increases the dew point effectiveness for all surface modifications. The performance of the capsule embossed HMX is closer to the corrugated regenerative HMX. Fig. 4.12 shows the variation of COP for all four types of plate surfaces in the HMX. The COP of the capsule embossed surface is the highest among all four types of regenerative HMX. The frictional loss of the corrugated surface is highest, which leads to its lowest COP among all types of surfaces. The COP and outlet temperature of the fin-type regenerative HMX is better than flat plate surface regenerative HMX. The difference in COP for all surfaces is wider at 45 ºC, and it gradually decreases at a lower inlet temperature. The exergy efficiency improves with the rise in the dew point depression, as shown in Fig. 4.13. The highest exergy efficiency is achieved for capsule embossed surfaces. The exergy efficiency of the corrugated surface is closer to the flat plate at a low dew point depression while it improves for the higher dew point depression. The increase in dew point depression increases the water consumption rate due to more scope of evaporation, but simultaneously, cooling capacity also increases. Hence water consumption rate per cooling capacity decreases with the increase of the wet-bulb depression, as shown in Fig.4.14. The water consumption rate of the capsule embossed surface and the corrugated surface is the lowest among all four

studied surfaces. The higher dew point depression increases the scope of the application of REC since performance is improved for all the investigating parameters.

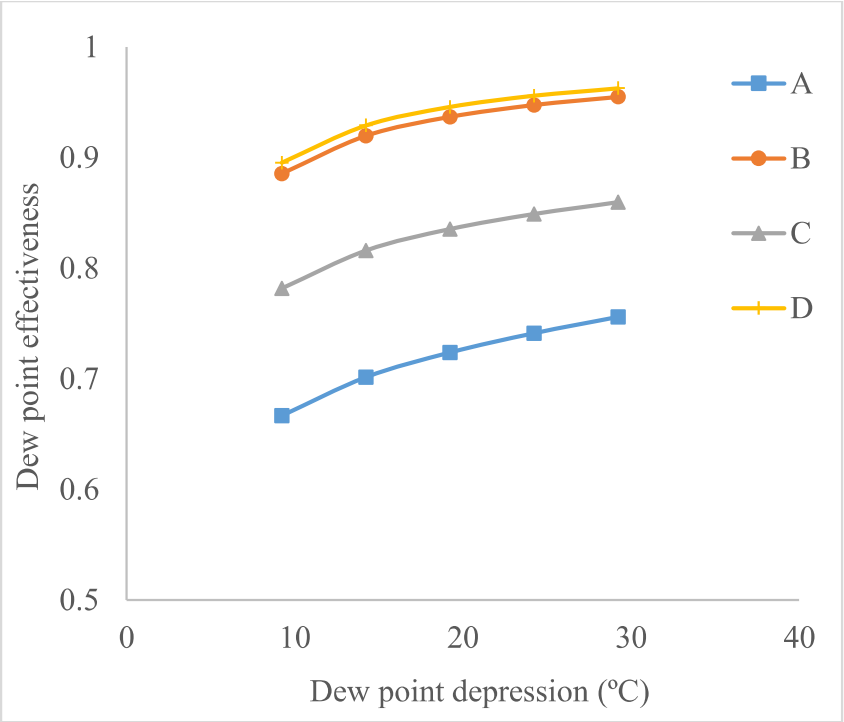

Fig. 4.10: Effect of dew point depression on dew point effectiveness

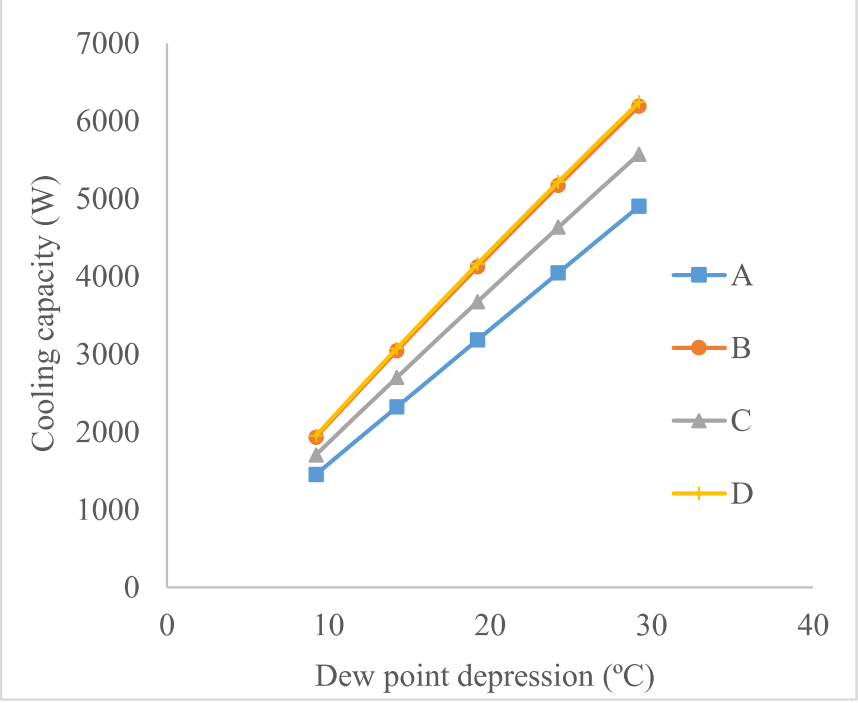

Fig. 4.11: Effect of dew point depression on cooling capacity

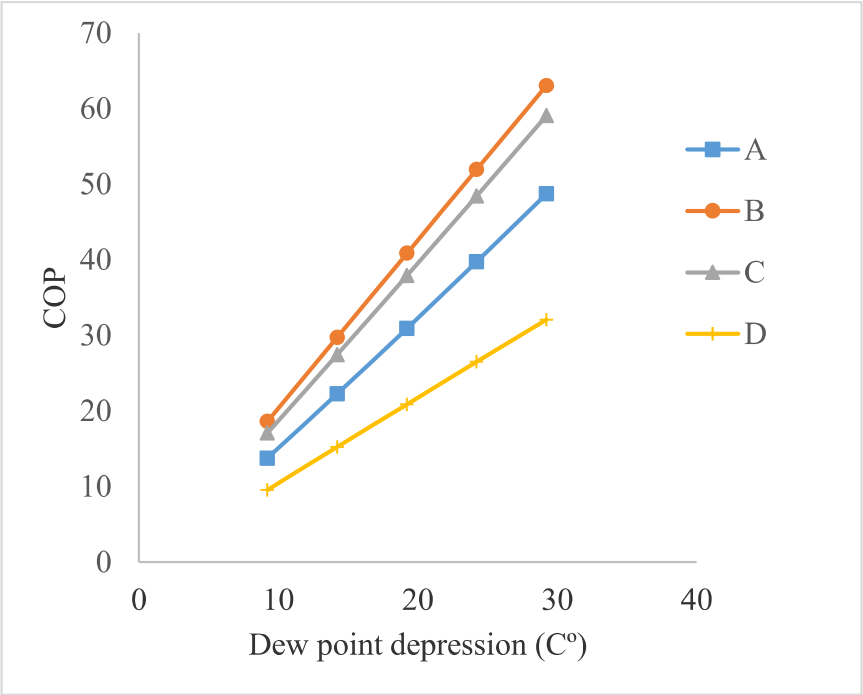

Fig. 4.12: Effect of dew point depression on COP

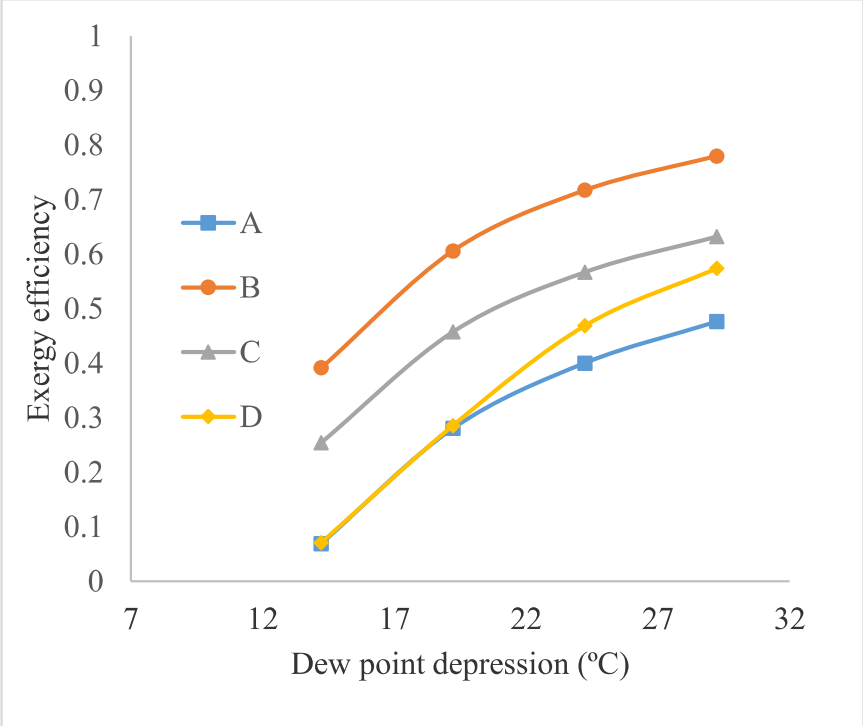

Fig. 4.13: Effect of dew point depression on exergy efficiency

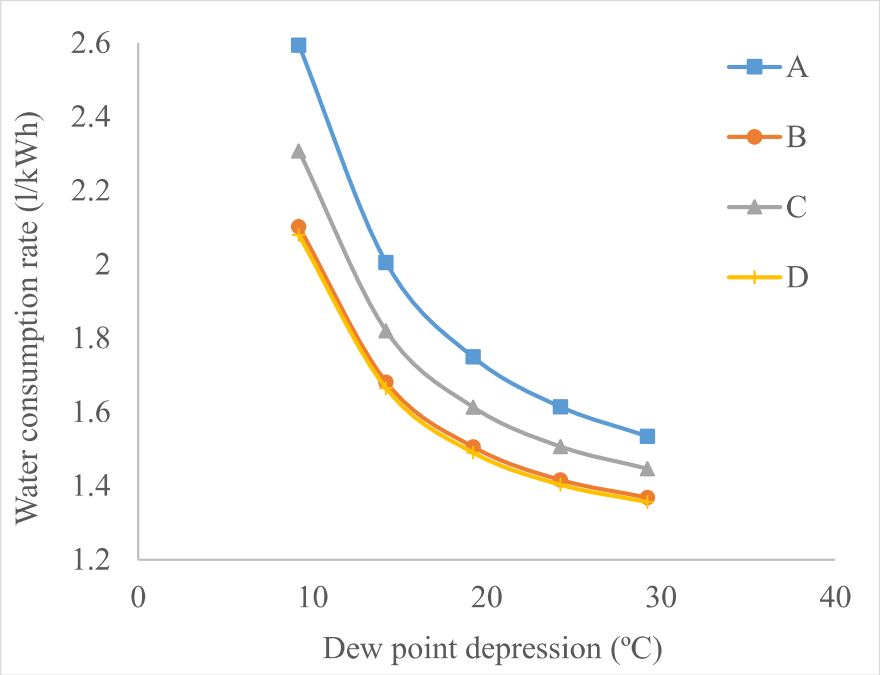

Fig. 4.14: Effect of dew point depression on the water consumption rate

4.3.3 Influence of inlet velocity

The increasing velocity of the dry air decreases the dew point effectiveness of all the four types of regenerative HMX, as shown in Fig. 4.15. This decrease is sharper for flat plate type while very slow for capsule type and corrugated surface type regenerative evaporative HMX. The increased velocity reduces the time to exchange heat, resulting in a reduction of temperature drop. It is obvious that the increased velocity increases the mass flow rate, which improves the cooling capacity of all cases. The higher intake velocity increases the mass of air in the dry channels of the regenerative evaporative coolers, which results in increased cooling capacity, as shown in Fig. 4.16. The dew point effectiveness of all HMX decreases while cooling capacity increases, so there needs to be a trade-off so that we can get cool air in the thermal comfort zone. The COP of all four types of regenerative HMX is shown in Fig. 4.17. The increased velocity increases the frictional loss, and it dominates the increased cooling capacity, which results in a reduction of COP. The fin adds surface and capsule embossed surface shows good COP results as compared to type A and type C. It is found that at a low velocity (1 m/s), the

cooling capacity of all four types of surfaces shows almost the same cooling capacity. The COP of all the four types of regenerative HMX converges at higher velocity (3m/s). The exergy efficiency of all four surfaces decreases with an increase in primary air velocity (Fig. 4.18). The variation of the corrugated surface and flat plate is almost similar. The exergy efficiency decreases drastically at a higher velocity. The exergetic performance of the finned surface lies between the corrugated and finned embossed surfaces. All investigated parameters converge at the lower dry air intake velocity except COP. The higher intake velocity ensures high cooling potential, but its temperature and power consumption need to be optimized as per the requirement and space to be cooled. The increase in primary air velocity increases the intake air volume flow rate. The wet channel air flow rate also increases, which leads to more evaporation of water. Hence, the water consumption rate increases with the increase of the primary air velocity (Fig. 4.19), but it is the lowest for capsule and corrugated surfaces. The difference in water consumption rate is significant at higher intake air velocity.

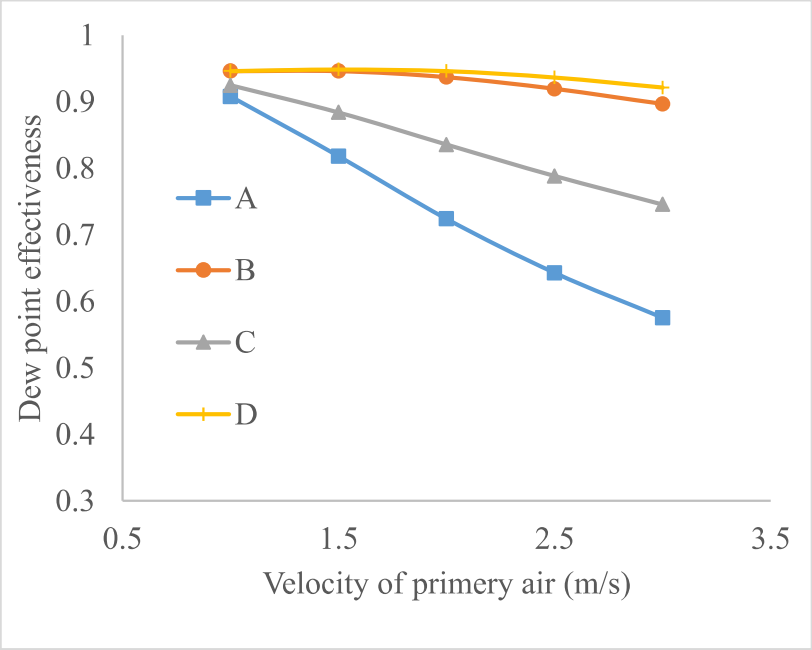

Fig. 4.15: Effect of primary air inlet velocity on dew point effectiveness

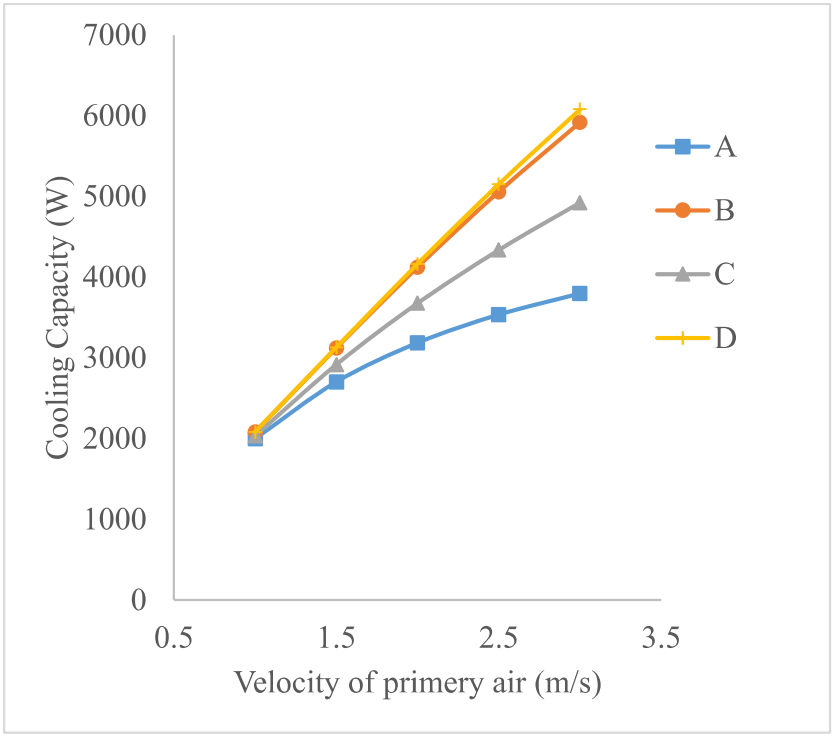

Fig. 4.16: Effect of primary air inlet velocity on cooling capacity

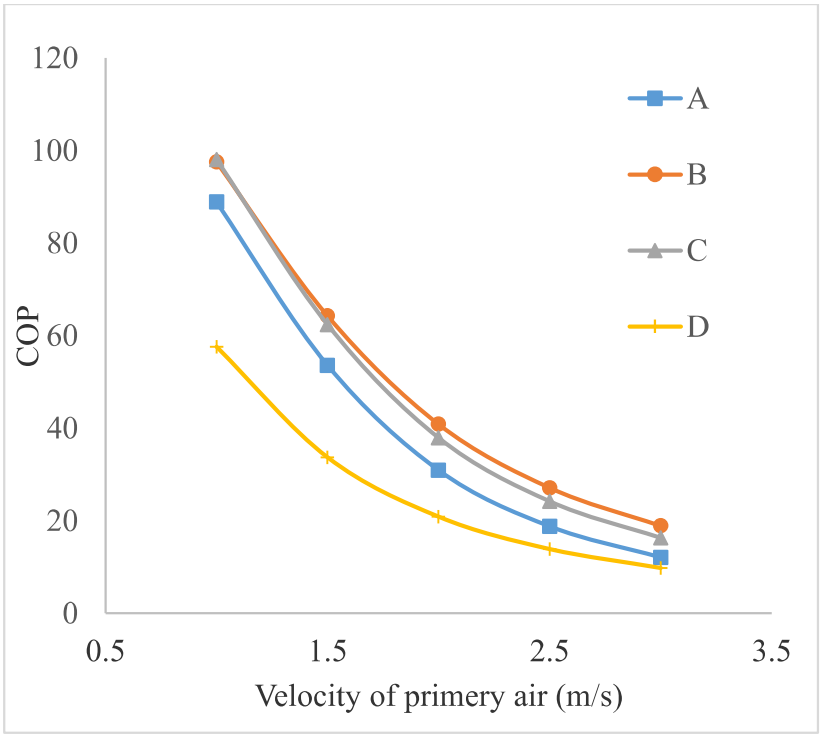

Fig. 4.17: Effect of primary air inlet velocity on COP

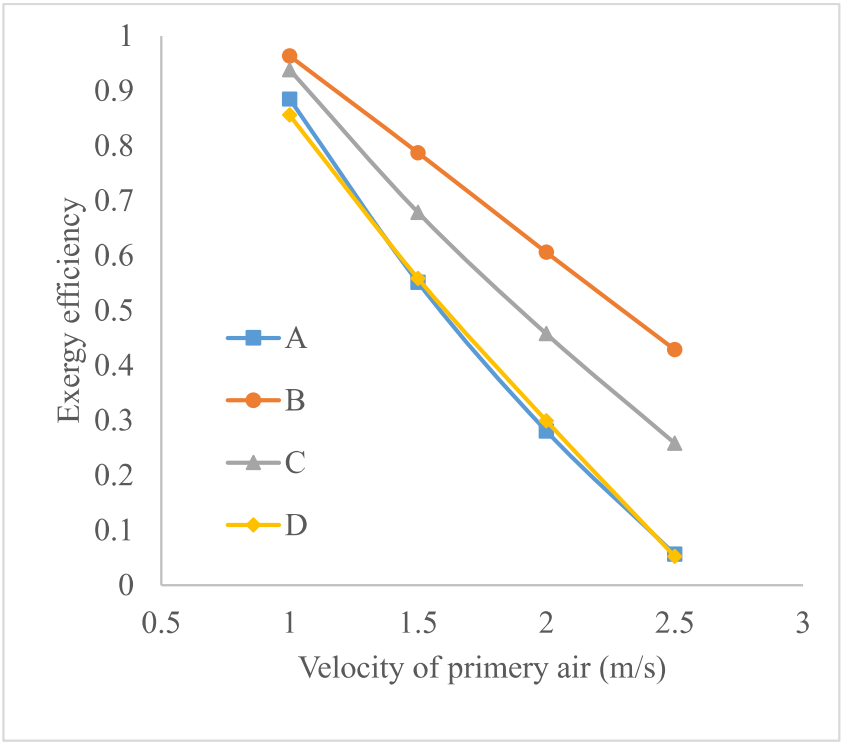

Fig. 4.18: Effect of primary air inlet velocity on exergy efficiency

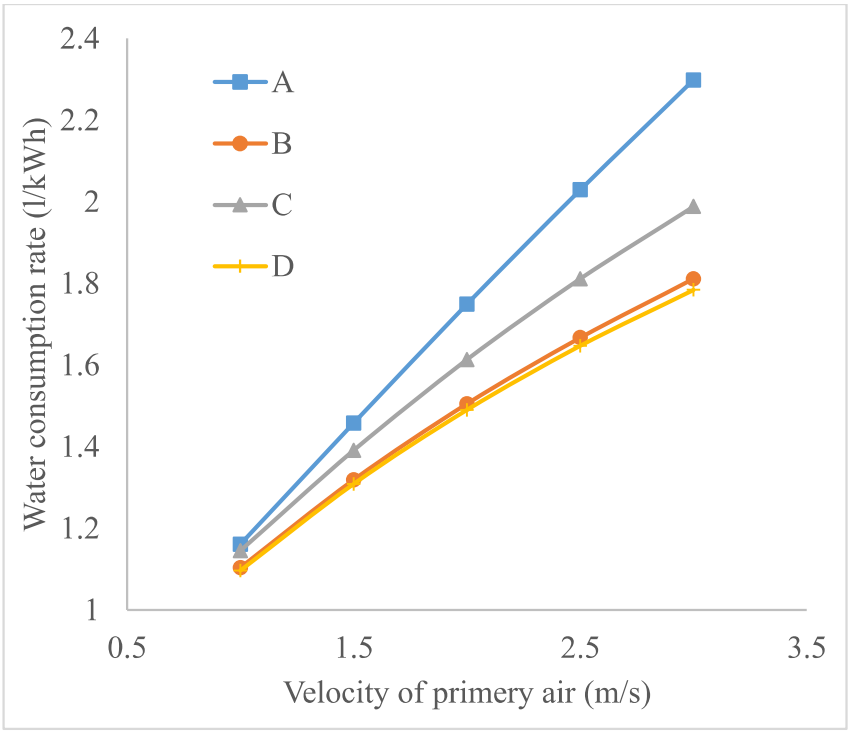

Fig. 4.19: Effect of primary air inlet velocity on the water consumption rate

4.3.4 Influence of water flow rate

The increase in the water flowrate first increases the dew point effectiveness; then, it starts decreasing for all four types of regenerative evaporative HMX. Dew point effectiveness is almost constant after a higher water flow rate, as shown in Fig. 4.20. The corrugated surface effectiveness shows the best result among all four. The cooling capacity of all four types of the surface increases up to 5 L/h then starts decreasing. This value depends upon the geometrical dimensions of the regenerative evaporative cooler. The cooling capacity is almost constant after a certain higher flow rate of the water. The COP of all four types of the surface first increases up to 5 L/h then starts decreasing sharply. The higher mass flow rate increases the power input of the regenerative device, which diminishes its COP (Fig. 4.21). The more mass of water creates additional resistance in heat transfer and increases the energy consumption of the water circulating pump too. The effectiveness (DPE) and cooling capacity of the corrugated plate HMX are highest, while its COP is lowest among all the modified surface heat exchangers. The fin-type regenerative HMX shows moderate performance, while capsule embossed HMX shows good performance in both (COP and effectiveness) the parameters. The exergy efficiency of all four modified surfaces increases as the circulating water flow rate increases. Fig. 4.22 shows improvement in exegetic efficiency at a higher flow rate since dew point effectiveness is also improved. The Exergetic efficiency of the corrugated surface is higher than the flat plate efficiency below the 5 L/h water flow conditions. The variation of the investigated parameters is sharp at a lower water flow rate while it is almost straight (approximately constant) at higher water flow conditions. The capsule embossed surface shows the highest Exergetic performance among all the analyzed surfaces.

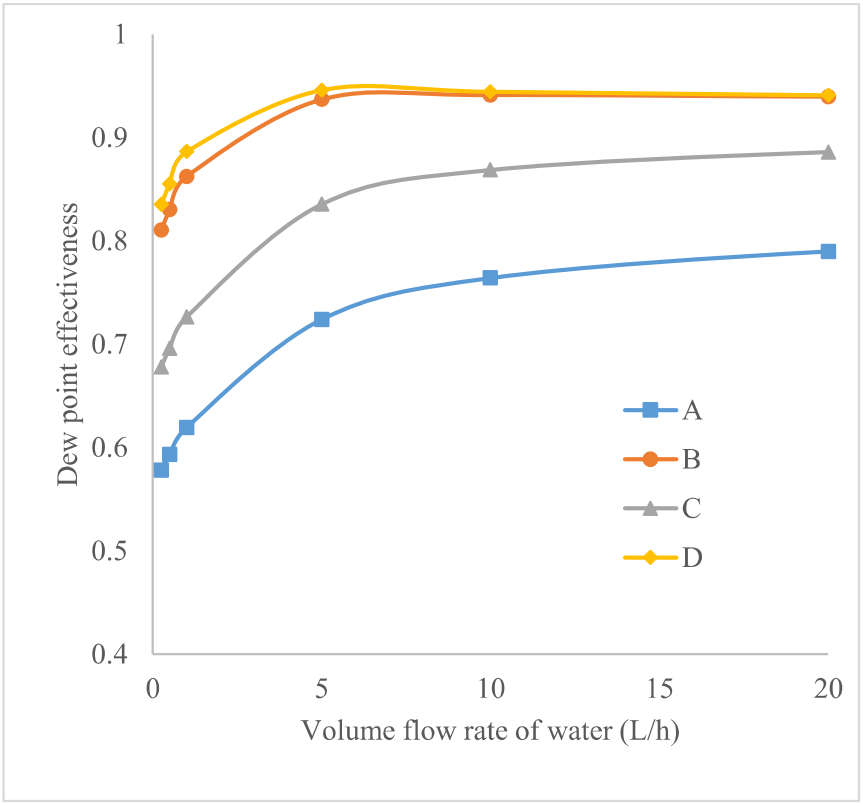

Fig. 4.20: Effect of water flow rate on dew point effectiveness

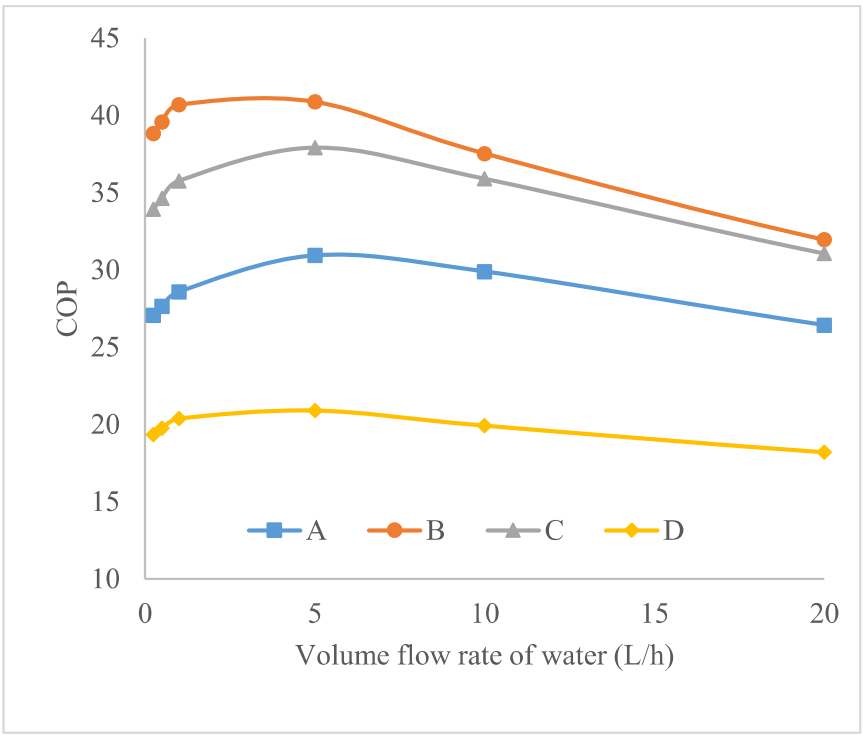

Fig. 4.21: Effect of water flow rate on COP

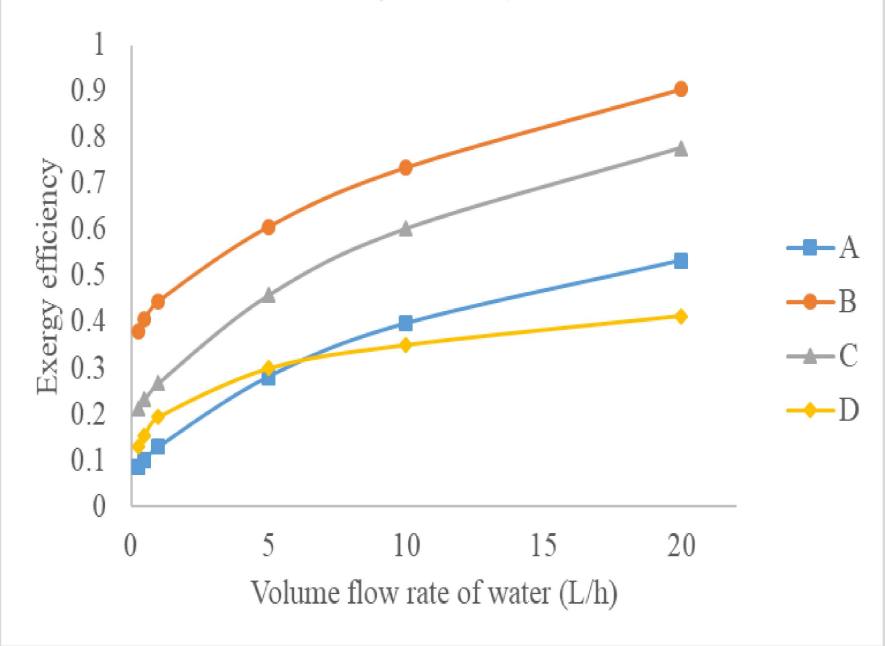

Fig. 4.22: Effect of water flow rate on exergy efficiency

The nanofluid (nanoparticles + water) is circulated in a close loop, passing through the pump, top water tank, wet channel, and bottom water tank. The supplied air (fraction of primary air going to cooling space) is not in direct contact with nanofluids, just exchanging heat in an indirect way, and hence there is no negative effect on the indoor condition. However, some challenges lie with the stability of the nanoparticle dispersion and safely cleaning of the tanks. Another important challenge to make it practically applicable is to refrain nanoparticles from forming aggregate during idling conditions of the cooling device. These challenges can be handled by the addition of surfactant and safety cleaning of the device. The same nanoparticles can be used for a long period of time to achieve economic heat transfer enhancement. The application of nanoparticles makes it a single-time investment to improve heat transfer. Since using different Nanofluids does not show much difference in the performance, then hybrid Nanoparticles should be selected based on cost and availability. Here, alumina and silicon carbide Nanoparticles are used to form hybrid nanofluid and further analysis. Preventive measures should be taken with the application of nanofluid in the device. There is

possibility that nanoparticle may escape to the air stream.There is very limited research that has been done on the filtrations of nanoparticles since it is not included in the standards of the ASHRAE and ANSI. It was found that less than diameter 10 nm is particle penetration tends to zero for good mechanical filtering media (Brochot et al., 2019). The filtration efficiency depends significantly on the velocity (Boskovic et al.,2008). The device can be easily designed to exit the wet channel at a lower velocity (wider cross-section). The fiberglass and high-grade HEPA (high-efficiency particulate air filter) show a filtering efficiency of 99.99 % for 3-20 nm of silver nanoparticles. The electrostatically charged polymer media is another option to filter nanoparticles without much affecting the flow. This filtrations process strongly depends upon particle charge. The combined filtration (mechanical + electrostatic) is another option to prevent escaping. The filtration adds additional resistance; hence pressure drops and fan work increase. The performance, especially COP of the device, needs to be investigated in these conditions. The use of nanofluid is not recommended after theoretical investigation of the evaporative cooler. This is because of a very marginal (almost negligible) improvement in the cooling performance and significantly increased initial cost of the device. The practical limitation also exists. The cooler utilizes cotton fabric as wetting media in the wet channels. This fabric is porous in nature which will create resistance for the nanoparticles. The nanoparticles will get trapped in this cotton fabric and making experimentation unfeasible. That's why this concept is restricted to theoretical analysis only.

4.4. Important findings

In this paper, counter-flow regenerative evaporative HMX has been studied with various heat transfer enhancement techniques. The analysis has been done on the application of different nanoparticles in the base fluid (water). The passive heat transfer enhancement techniques such as capsule embossing, finned surface, and corrugated

surface on the dry side of the HMX is investigated. A comparative study has been done for four types (flat, capsules embossed, finned, and corrugated) of the plate surfaces. The performance of the above- surfaces is studied under various operating conditions. The main findings can be summarised as follows:

- After carrying out a theoretical analysis of the evaporative cooler, the usage of nanofluid is not advised. The only use of hybrid nanofluid as a coolant in the regenerative HMX is not much fruitful as it yields marginal improvement, while its application with plate surface modification provides a significant amount of enhancement in terms of all considered performance parameters.
- The cooling capacity for the corrugated surface is highest among considered plate surfaces and increases with an increase in dew point depression, air velocity, and water flow rate.
- The dew point effectiveness is highest for corrugated surfaces and increases with an increase in water flow rate and dew point depression, and a decrease in air velocity.
- COP of the capsule embossed surface is highest and 10 % higher than flat plate at 1 m/s velocity of primary air. It increases with increases in the dew point depression and decrees in air velocity.
- The water consumption rates of the corrugated and capsule embossed surfaces are almost equal and lowest among all modified surfaces.
- The exergy efficiency of the capsule embossed surface is better as compared to other plate surfaces and increases with water flow rate and dew point depression.
- The optimized water flow rate is found around 5 L/h for all the four plate surfaces used in the present study to get maximum cooling capacity, effectiveness, and COP.
- The capsule embossed surface is found best among all the considered plate surfaces of REC in terms of COP and exergy efficiency.

This page is intensionally left blank